Neutron-proton $l = 0$ scattering

Thomas Redpath and Dayah Chrisman[1]
[1]*Department of Physics, Michigan State University*

We solve the Lippman-Schwinger equation for proton-neutron scattering to obtain the $l = 0$ phase shift δ_0 as a function of lab energy. We use a sum of three Yukawa potentials with empirically derived parameters to approximate the *np* interaction and set up a matrix equation for the reaction matrix. We solve this matrix equation numerically to extract δ_0. Our results agree with the experimental phase shifts tabulated in Stoks et al. [2] to within 10% for lab energies at or below 100 MeV. Furthermore, our calculations are stable with 50 mesh points.

INTRODUCTION

Measuring the final states of two nucleons after they interact provides information about the nature of their interaction. One way to summarize the information we get from these scattering experiments is through the phase shift - which can be roughly described as a shift in the scattered wavefunction relative to the incoming one. In this project, we study the behavior of the $l = 0$ phase shift (δ_0) as a function of energy for a toy neutron-proton (np) interaction model.

Qualitatively, we say that a repulsive potential will result in a negative phase shift - the scattered wavefunction is "pushed out" and that an attractive potential will give a positive phase shift. Thus by analyzing experimental data we can deduce whether a potential is repulsive, attractive, or a mixture of both. The nuclear potential is negligible at long ranges ($r >$ a few fm), attractive at intermediate ranges ($r \sim 1$ fm) and repulsive at very short distances ($r < 0.5$ fm). By examining the phase shift as a function of energy, we can see at which energies the incoming particle is "repelled" (giving a negative phase shift). This can give us an idea of the range of the repulsive inner part of the potential, since the particle needs enough energy to approach the inner, repulsive part of the potential.

We organize this report as follows: first we summarize the algorithms we need to solve the problem numerically. We then describe the framework we used to carry out our calculations. Next, we present the results of our calcuations and some qualitative insights derived from considering the variable phase approach. Finally, we summarize our findings and offer some comments about possible extensions of our framework.

THEORY AND ALGORITHMS

Lippman-Schwinger Equation

In order to calculate the phase shifts δ_l, we need to solve the Schrödinger equation for the neutron-proton system with $E > 0$. This can be expressed as an integral equation for the reaction matrix

$$R_l(k,k') = V_l(k,k') + \frac{2}{\pi}\hat{P}\int_0^\infty dq q^2 V_l(k,q)\frac{1}{E - q^2/m}R_l(q,k'), \quad (1)$$

where $E = k_0^2/m$ is the total kinetic energy of the nucleons in the center-of-mass system and the momentum-space representation of the potential $V(k',k)$ is used. We solve this equation numerically on a discretized domain where we've set the mesh points and weights using Gaussian Legendre quadrature. We map the points and weights from the interval of the Legendre polynomials ($x \in [-1,1]$) to our desired interval $r \in [0,\infty)$ using the following mapping

$$k_i = const \times tan\left\{\frac{\pi}{4}(1+x_i)\right\}$$
$$\omega_i = const\frac{\pi}{4}\frac{w_i}{cos^2\left(\frac{\pi}{4}(1+x_i)\right)}.$$

We summarize the prescription for solving eq. 1 numerically from Bogner and Hjorth-Jensen [1]. First, we employ Cauchy's principle-value prescription to re-write eq. 1 in the form

$$R(k,k') = V(k,k') + \frac{2}{\pi}\int_0^\infty dq \frac{q^2V(k,q)R(q,k') - k_0^2V(k,k_0)R(k_0,k')}{(k_0^2 - q^2)/m}, \quad (2)$$

which is represented on the discretized mesh as

$$R(k,k') = V(k,k') + \frac{2}{\pi}\sum_{j=1}^N \frac{\omega_j k_j^2 V(k,k_j)R(k_j,k')}{(k_0^2 - k_j^2)/m} - \frac{2}{\pi}k_0^2V(k,k_0)R(k_0,k')\sum_{n=1}^N \frac{\omega_n}{(k_0^2 - k_n^2)/m}, \quad (3)$$

where there are N mesh points from the Gaussian quadrature mapping and one point that is the chosen "observable" point corresponding to the relative momentum for which we want to calculate the phase shift. In total there are $(N+1)$ mesh points.

Next, we organize eq. 3 as a matrix equation by defining a matrix A

$$A_{i,j} = \delta_{i,j} - V(k_i, k_j)u_j$$

where

$$u_j = \frac{2}{\pi}\frac{\omega_j k_j^2}{(k_0^2 - k_j^2)/m} \qquad j = 1, N \tag{4}$$

and

$$u_{N+1} = -\frac{2}{\pi}\sum_{j=1}^{N}\frac{k_0^2\omega_j}{(k_0^2 - k_j^2)/m}. \tag{5}$$

We can now solve for the R matrix by inverting the matrix A and multiplying V by A^{-1}. Finally, the $R(N+1, N+1)$ element is related to the phase shift for k_0 by

$$R(k_0, k_0) = -\frac{tan\delta}{mk_0} \tag{6}$$

Using this prescription and some model for the interaction (see next subsection), we can calculate δ for scattering at some incident energy. We describe the `C++` code used to make these calculations in the Methods section.

Potential Model

We currently have coded two potentials that can be used in the phase shift calculation. The first is a finite square well (eq. 7) used to benchmark the program against the analytical result. The second is a parameterized $^1S_0$ neutron-proton interaction (eq. 8).

$$V = -V_0\Theta(a - r) \tag{7}$$

$$V(r) = V_a\frac{e^{-ax}}{x} + V_b\frac{e^{-bx}}{x} + V_c\frac{e^{-cx}}{x}, \tag{8}$$

with $x = \mu r$, $\mu = 0.7$ fm^{-1} (the inverse of the pion mass), $V_a = -10.463$ MeV and $a = 1$, $V_b = -1650.6$ MeV and $b = 4$ and $V_c = 6484.3$ MeV and $c = 7$.

For both potentials, we find the momentum-space representations using the Fourier-Bessel transform, we specialize to the case $l = 0$ since we're only aiming to calculate δ_0. For the finite well potential we have

$$\begin{aligned} V_l(k, k') &= \int j_l(kr)V(r)j_l(k'r)r^2dr \\ &= V_0\int_0^a \frac{\sin(kr)\sin(k'r)r^2}{kk'r^2}dr \\ &= \frac{V_0}{kk'}\int_0^a \sin(kr)\sin(k'r)dr \\ &= \frac{V_0}{kk'}\frac{k'\sin(ka)\cos(k'a) - k\cos(ka)\sin(k'a)}{k^2 - k'^2} \end{aligned}$$

and

$$V(k, k) = \frac{V_0}{k^2}\left(\frac{a}{2} - \frac{2\sin(ka)}{4k}\right)$$

in the case $k = k'$. For the np model, the momentum space representation is

$$V(k, k') = \frac{V_\eta}{4\mu kk'}\ln\left[\frac{(\mu\eta)^2 + (k + k')^2}{(\mu\eta)^2 + (k - k')^2}\right]$$

A Matrix

Care must be taken when setting up the matrix A to solve for the reaction matrix. Pedantically, there are four sections of this matix that must be treated separately.

1. $A(i, j) = \delta_{i,j} - V(i, j)u_j$ for $i, j \in 1..N$
2. $A(N+1, j) = -V(N+1, j)u_j$ for $j \in 1..N$, the last row
3. $A(i, N+1) = -V(i, N+1)u_{N+1}$ for $i \in 1..N$, the last column
4. $A(N+1, N+1) = 1 - V(N+1, N+1)u_{N+1}$ bottom right corner

METHODS

We implemented our numerical solution to the Lippman-Schwinger equation as a `C++` class. This class consists of three two-dimensional data structures to hold the V, A and R matrices, two one-dimensional data structures to hold the weights and momentum mesh points that define the integration domain and several ancillary variables that specify the nucleon mass and other book-keeping parameters. Application of the algorithms sketched in the previous section is carried out in a series of member functions that (a) set up the mesh points and weights (b) set up the potential matrix (c) set up the A matrix (d) invert A to get R then extract δ_0. In principle, different functions may be used to set up different potentials; we coded one for the model np interaction given above and one for a finite spherical well to

check that we recover the analytic result. This class is defined in the source files `NucleonScattering.cpp` and `NucleonScattering.hh`. An instance of the class is created and the correct sequence of methods is called in the `main` function defined in `main.cpp`. We include three versions of `main.cpp` that (1) calculate δ_0 for a single energy, (2) loop over energies and calculate δ_0 for the a range of energies using the finite spherical potential and (3) run the calculation for the experimental energies. The results from cases (2) and (3) are saved to the files `output/FiniteSpherel0ps.txt` and `output/l0ps.txt` repectively. We generated FIG. 1 and FIG. 2 from these files.

RESULTS AND DISCUSSION

As a check, we calculate δ_0 from the analytic formula for the simple finite square well.

$$\delta_0(E) = \arctan\left[\sqrt{\frac{E}{E+V_0}}\tan\left(R\sqrt{2\mu(E+V_0)}\right)\right] - R\sqrt{2\mu E} \tag{9}$$

where

$$E = \frac{k^2}{2\mu}$$

The results are shown for three different numbers of mesh points ($N = 5, N = 50, N = 100$) in FIG. 1. In terms of convergence, our result is stable with $N = 50$ points. The overall agreement with the analytic result is worse for higher lab energies because there are fewer mesh points at these higher energies. The way we map our integration points from the interval $[-1, 1]$ to $[0, \infty)$ results in a higher density of mesh points at lower energies. Therefore, we expect the calculation to be more accurate at lower energies. FIG. 1 shows that our results agree with the analytic value to within 25% for E_{lab} less than 100 MeV.

In FIG. 2, we plot our calculated phase shifts next to the experimental results tabulated in [2]. For lab energies at and below 100 MeV, we see good agreement with the data ($< 10\%$), suggesting that our model potential best reproduces the underlying physics at lower energies. The model also reproduces the point ($E_{\text{lab}} = 250$ MeV) where δ_0 turns negative and we start to probe the repulsive core of the interaction.

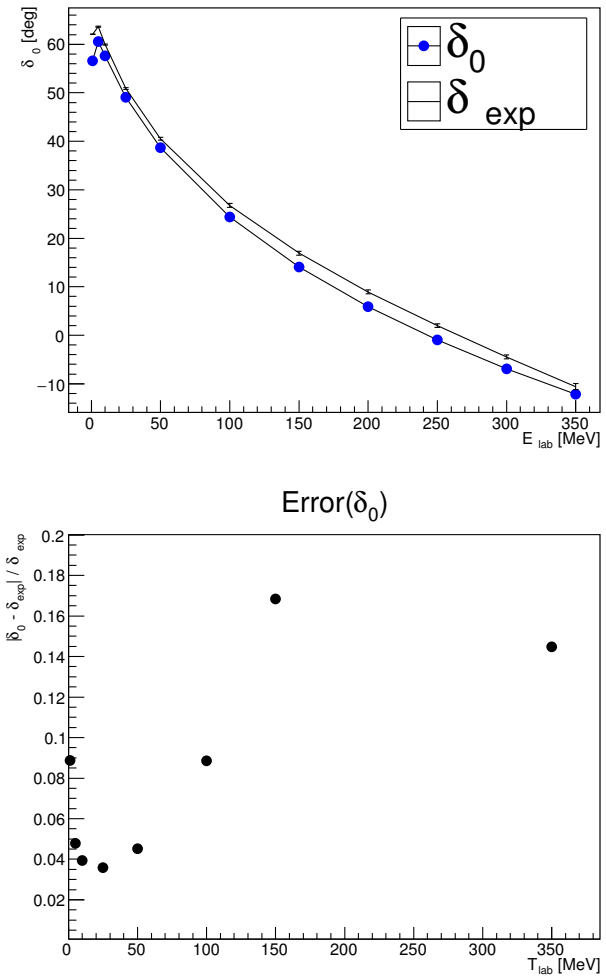

FIG. 2. A comparison of δ_0 calculated with our code (blue points) to the experimental values tabulated in [2] (error bars). The top panel shows the phase shifts in degrees and the bottom panel plots the % difference between our calculated values and the tabulated experimental results. We used 50 mesh points for the calculation.

Variable Phase Approach

The variable phase approach (VPA) relies on numerical methods to solve the differential equation.

$$\frac{d\delta(k,r)}{dr} = -\frac{1}{k}2MV(r)\sin^2[kr + \delta(k,r)]$$

for $\delta(k, r)$. The VPA is simple to use, and information about the potential is relatively easy to extract. For example, here we show that the presence of bound states (and the number of them) for a certain potential depth can be quickly determined, and short-range repulsive components of the potential can be inferred based on phase shift calculations at various energies.

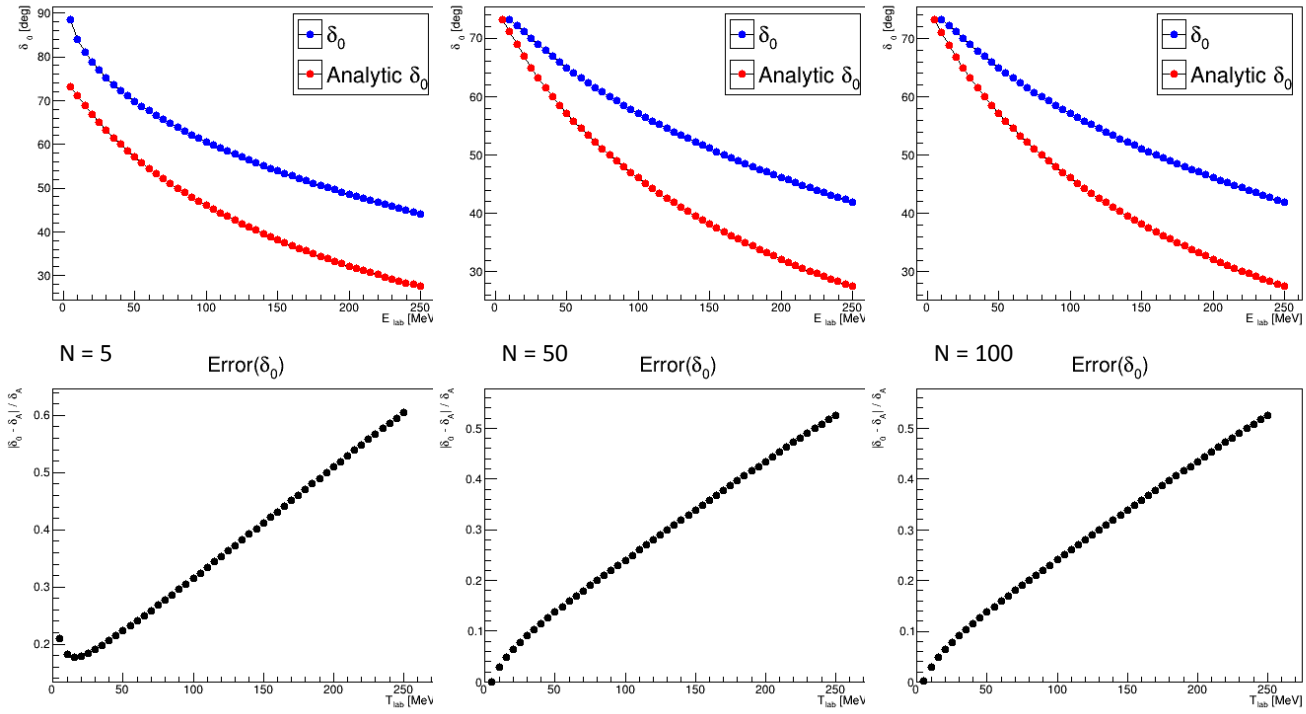

FIG. 1. Results for the finite square well ($V_0 = -0.5$ fm^2, $a = 1.$ fm) $l = 0$ phase shifts as a function of lab energy. In each plot, our calculations are represented by the blue points and the analytic results are plotted in red. The black points in the lower plots show the deviation of our calculation from the analytic result. From left to right we plot the results of our calculation for N=5, N=50 and N=100 to show convergence for 50 mesh points.

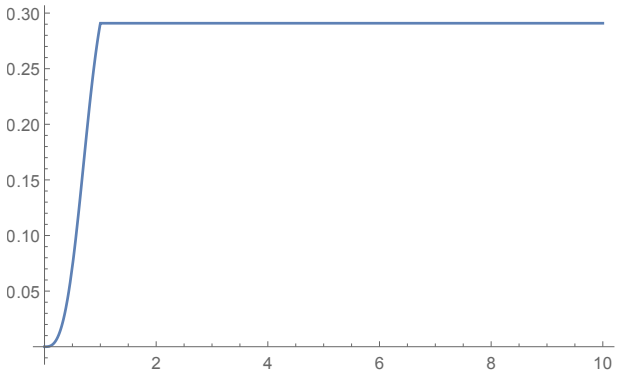

FIG. 3. Phase shift as a function of radius.

The VPA truncates a realistic potential at some cutoff radius ρ. Then, we inegrate over r out to a sufficiently large radius ($R_{\max} > \rho$).

In FIG. 3, we note that the phase shift becomes constant after a radius of 1; this is the radius of the square well potential we used. Because of the discontinuity in the potential at the edge of the square well, there is no ambiguity about how large we need to make our integration radius: obviously, as soon as we are looking beyond the radius of potential, the phase shift will converge to a constant value. This tells us that an integration radius greater than the square well will be sufficient for the phase shift to converge.

We then examined the plots of $k\cot(\delta)$ and δ to test Levinson's Theorem, which states that the number of bound states can be calculated by looking at $\delta(E = 0)$ and the limit of δ as E approaches ∞

$$\phi_l(0) - \phi_l(\infty) = n\pi$$

where n is the number of bound states the potential can hold. For a well depth $V_c = 1.0$, $\phi_l(0) = 0$, $\phi_l(\infty) = 0$. This means that this well cannot bind any states with $l = 0$. For a well depth $V_c = 2.0$, $\phi_l(0) = 3.14$, $\phi_l(\infty) = 0$, meaning that at this depth, the well can hold one $l = 0$ bound state.

We add now a short-range repulsive potential and calculate the phase shifts using the VPA.The sign of the phase shift can characterize a potential as attractive ($\delta_0 > 0$) or repulsive ($\delta_0 < 0$). Adding a repulsive term should begin to make a difference at higher energies where the approaching particles can get close enough to "see" the effect of the repulsive core. At these higher energies, we should see the phase shift turn negative, indicating the repulsive character of the potential.

With $V_c = 0$ there is no repulsive part and the potential is purely attractive, we get that $\phi_l(\infty) = 0$. This indicates, as we predicted, a purely attractive potential. Around $V_c = 18$, we can see the phase shift turning over at around $k = 10$. As we increase the height of the repulsive potential, the phase shifts start to become negative at lower and lower energies, until at $V_c = 100$ the phase shift turns negative at only $k = 6$.

Because the nuclear force is repulsive at short distances ($V \to \infty$ for $r \to 0$), we can use calculated phase shifts from experimental cross sections to estimate the range of the repulsive part of the nuclear force (R_c). The incoming momenta/energy (k) at which the phase shift changes gives us an estimate of the length scale at which the repulsive piece of the interaction becomes dominant.

CONCLUSIONS

In this project, we solved the Lippmann-Schwinger equation numerically to compute the $l = 0$ phase shifts for a model np potential. Our calculations are stable with $N = 50$ mesh points. We see decent agreement with experimental data suggesting that our model does a reasonable job of describing the underlying physics. Furthermore, we explored the variable phase approximation to gain an intuitive understanding of the relationship between the sign of δ_0 and the sign of the potential. The VPA also provides us with a simple framework to demonstrate Levinson's theorem.

We can easily incorporate any potential model into this framework by coding the appropriate form of the potential. In this way, we could extend our analysis to higher values of l or other models for the interaction.

[1] S. Bogner and M. Hjorth-Jensen. Non-relativistic and relativistic scattering theory. url = https://manybodyphysics.github.io/NuclearForces/, Oct 2017.

[2] V. G. J. Stoks, R. A. M. Klomp, M. C. M. Rentmeester, and J. J. de Swart. Partial-wave analysis of all nucleon-nucleon scattering data below 350 mev. *Phys. Rev. C*, 48: 792–815, Aug 1993. doi:10.1103/PhysRevC.48.792. URL https://link.aps.org/doi/10.1103/PhysRevC.48.792.